Structural and electronic transformations of liquid selenium at high temperature and pressure: A ^{77}Se NMR study

William W. Warren, Jr.
Bell Laboratories, Murray Hill, New Jersey 07974

R. Dupree
University of Warwick, Coventry, England
and Bell Laboratories, Murray Hill, New Jersey 07974

(Received 12 March 1980)

Liquid Se has been investigated by ^{77}Se NMR from the supercooled liquid (193 °C) to the supercritical fluid (1625 °C) and at pressures up to 790 bars. The resonance shifts and nuclear relaxation observed between roughly 400 and 1550 °C are attributed to paramagnetic centers at the polymeric chain ends. The data yield the chain-end hyperfine coupling $A = 2.87 \pm 0.24 \times 10^{-18}$ ergs, the enthalpy of chain scission $\Delta H_{sc} = 31.6 \pm 1.5$ kcal/mole, and the activation volumes for scission. The inferred average degree of polymerization decreases from about 750 atoms per molecule at 600 °C to about 7 atoms at 1550 °C. With increasing concentrations of paramagnetic centers, the electron-spin correlation times shorten rapidly to about 5×10^{-14} s at 1550 °C. Application of pressure at 1550 °C induces a rapid delocalization of the paramagnetic centers which coincides with the Mott minimum metallic conductivity. The supercritical vapor is strongly paramagnetic with a susceptibility $\sim 1 \times 10^{-4}$ emu/g atom.

I. INTRODUCTION

Elemental selenium melts to form a liquid of unique and often striking properties. The twofold coordination in helical chains of trigonal crystalline Se is largely preserved on melting in the form of linear-chain polymers. Yet unlike sulfur, which it resembles in many respects, Se possesses low-lying unoccupied electronic states which imbue it with semiconducting electronic properties near the melting point (T_m). Because of the preservation of twofold coordination the electronic structure of liquid Se near T_m is similar to those of the crystalline and amorphous solid forms. As an elemental liquid, Se is an example of a liquid semiconductor in which the chemical bonding is purely covalent.

The special character of liquid Se can also be seen when its properties are considered in relation to the other liquid chalcogen elements. The lightest chalcogen, oxygen, forms diatomic molecules and is a pale blue insulator. Next, in order of increasing atomic weight, is sulfur which initially melts to form a light yellow insulating liquid of S_8 rings. However, at about 40 K above T_m the structure transforms abruptly to large polymeric chains. At sufficiently high temperatures sulfur behaves like an electronic semiconductor.[1] Selenium, the third chalcogen is a semiconductor at T_m with a polymeric structure similar to that of sulfur above the polymerization temperature. The fourth element, tellurium, is a poor metal in the liquid state and the structure is believed to contain a large fraction of threefold coordinated sites. Finally, polonium exhibits roughly sixfold bonding and is a liquid metal. Thus Se embodies both the low coordination and tendency for molecule formation of the lighter chalcogens and the electronic conduction properties of the heavier elements.

The properties of Se are especially interesting when considered over ranges of temperature and pressure sufficiently wide to include the liquid-gas critical point and the supercritical fluid ($T_c = 1590 \pm 20$ °C, $P_c = 380 \pm 30$ bars).[2] It is evident that there must occur radical modifications of the fluid structure under these conditions. The dilute vapor consists mainly of small molecular species such as Se_2, yet it is accessible from the polymeric liquid by continuous variation of temperature and pressure over the critical point. These structural changes can be expected to be accompanied by significant modifications of the electronic structure and properties. The continuous nature of the structural and electronic transformations provides a special opportunity to investigate the relation between structure and electrical and magnetic properties in a disordered system.

Until recently virtually nothing was known of the structural and electronic properties of liquid Se far from the normal liquid range. The first experimental indications of the electronic transformations are found in the electrical conductivity data obtained by Hoshino *et al.*[2,3] near the critical point and in the su-

percritical fluid. It was found that the semiconducting properties give way to an insulating state in the immediate vicinity of the critical point. In contrast, application of relatively modest pressures (1–2 kbar) near the critical temperature produces a *metallic* state whose conductivity approaches that of normal liquid Te. Thus at high temperature and pressure, the fluid can be induced either to behave more like oxygen and sulfur or like tellurium and polonium by appropriate changes in the experimental conditions. These transformations of the electrical properties are summarized on the P-T phase diagram shown in Fig. 1 on which contours of constant dc conductivity are superimposed.

The present nuclear magnetic resonance (NMR) investigation was undertaken with the intention, first, of determining more specific details of the structural evolution of fluid Se up to the supercritical region and, second, of observing from a microscopic vantage point the electronic transformations which accompany these structural changes. NMR enjoys a special advantage with regard to the latter goal because of its strong sensitivity to local static and dynamic magnetic fields. Such fields can be anticipated at the nuclei as a result of the spins of unpaired localized and itinerant electrons. The experiments covered the full range of temperature from below the melting point to the supercritical fluid and they extend to a pressure of 800 bars where incipient metallic behavior is observed. Our measurements include resonance shifts produced by electronic paramagnetism and nuclear relaxation rates related to the microscopic electronic and structural dynamic properties.

The remaining portion of this paper is organized as follows. Section II describes details of our experimental methods and apparatus. The experimental results are presented in Sec. III. Section IV begins with a brief summary of the known structural and electronic properties of liquid Se followed by analysis and interpretation of our data for the semiconducting polymer region (Sec. IV B), the region of the semiconductor to metal transition (Sec. IV C), and the insulating supercritical fluid (Sec. IV D). Finally we present in Sec. V a brief summary and the main conclusions of our work.

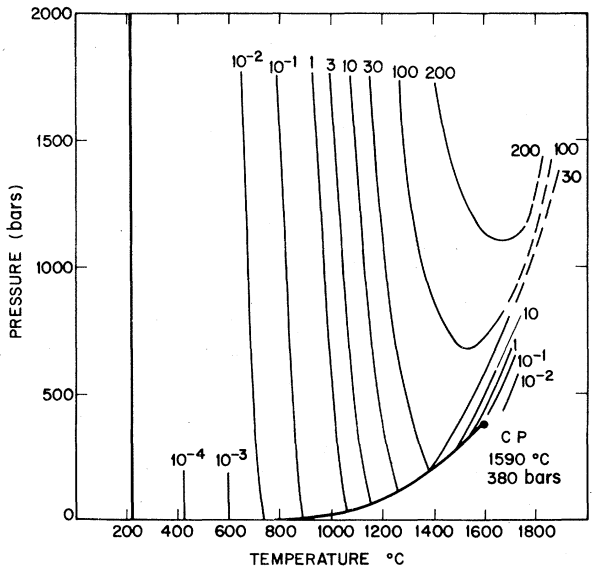

FIG. 1. Pressure-temperature phase diagram of selenium showing contours of constant dc electrical conductivity in liquid and supercritical fluid (after Endo *et al.*, Ref. 64). Data from Refs. 2, 3, and 75.

II. EXPERIMENTAL APPARATUS AND METHODS

The experiments required sample environments throughout the temperature range from the Se melting point (217 °C) to roughly 1600 °C and, concurrently, under hydrostatic pressure up to 800 bars. These conditions were achieved within an internally heated Be-Cu autoclave pressurized with argon gas. The required temperatures were obtained with a cylindrical heating element made of Mo wire wound noninductively on an alumina form. The entire high-temperature zone was insulated from the walls of the pressure vessel by a laminated structure formed by alternating layers of zirconia cloth and Mo foil. The purpose of the lamination was to minimize thermal conduction in the radial direction while suppressing convection in the compressed argon gas. A Mo sample coil for NMR was wound on a cylindrical alumina form which fitted into the heating element and whose inner diameter just accepted the cell containing the liquid Se sample.

The sample cell assembly is illustrated in Fig. 2. A Lucalox measurement cell was connected by a capillary to a small reservoir made of alumina. The ceramic components were cemented together with a

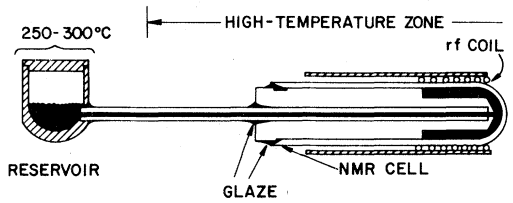

FIG. 2. Experimental cell for NMR studies of liquid selenium in an internally heated autoclave. Heavy shading, liquid selenium; light shading, alumina; unshaded, Lucalox. Nongas-tight cap on reservoir permitted pressure equilibration between selenium and pressure medium (argon gas). Lucalox filler in center of NMR cell reduced amount of enriched ^{77}Se sample material required.

high-temperature glaze.[4] The reservoir provided a means of initially filling the measurement cell and allowed for expansion when the sample was heated to the region of the critical point. The reservoir was contained within a small box of solid copper which was maintained, by means of a heater on its outer surface, at a temperature some 50 to 100 degrees above the melting point of Se. As the need for pressure equilibration within the cell dictated that the reservoir not be gas tight, the use of a copper box had the additional advantage that escaping Se vapor reacted with the inner copper surface thus reducing Se contamination elsewhere within the pressure vessel.

The following procedure was followed to fill the measurement cell with molten Se. During assembly of the autoclave, the reservoir was loaded with solid Se. After closing the high-pressure seals, the entire assembly was evacuated and the main heater was turned on to bring the measurement cell to a temperature of about 300 °C. Then, still under vacuum, the reservoir was heated to 250–300 °C to melt the Se. Finally, the autoclave was pressurized with 3–5 bars which was sufficient to force molten Se through the capillary and fill the measurement cell. Entrance of Se into the cell was easily detected by a sharp change in the rf tuning characteristics of the NMR coil. Once the cell had been filled, the temperatures of both reservoir and measurment cell were maintained above the Se melting point throughout the experimental run.

Because of the low natural abundance of ^{77}Se (7.5 at.%), it was necessary to use isotopically enriched material to achieve adequate signal-to-noise ratios at high temperature. The material used in these experiments was enriched to 94.38 at.% ^{77}Se.[5] As supplied, the enriched Se was of relatively low chemical purity. The results of spectrographic analysis supplied with the material indicated a possible Zn concentration of as high as 0.2 at.% and the upper limits on the concentrations of numerous other metal impurities were in the range 100–500 ppm. Our initial attempt to melt the enriched Se in a sealed quartz ampoule resulted in an explosive rupture of the cell when the material melted. We attribute this to chemical reaction of the Se with metal impurities. As a result of this experience, we routinely purified the enriched material by vacuum distillation before any measurements were attempted. The distillation was repeated for material recovered following each experimental run.

Sample temperatures in the autoclave were controlled by means of a Pt vs Pt–10 at.% Rh thermocouple located about 1 mm from the closed end of the sample cell. The thermocouple output was used to generate an error signal in a regulation loop controlling the power supplied to the heating element. Because of sharp thermal gradients associated with convection in the argon at high pressures, this thermocouple did not provide sufficiently accurate readings of the temperature of the sample itself. Therefore the resistance of the Mo NMR coil was used as a secondary thermometer. The coil was in close contact with the outer wall of the measurement cell and was located in a region of relatively low convection. The thermometers were calibrated against the vaporization point at 100 bars ($T_v = 1270 \pm 10$ °C) using the vapor pressure data of Hoshino, Schmutzler, and Hensel.[2] Vaporization of the Se sample was readily detected as an abrupt loss of NMR signal and change in the Q of the rf coil as the sample was heated through the transition. The absolute accuracy of temperature measurements in the vicinity of this calibration point was ± 20 °C. The estimated error of temperature measurements relative to this point increased from zero at 1270 °C to possibly as much as ± 20 °C at 1600 °C. In the low-temperature range, the convection effects were less serious so that the correction of the thermocouple reading was relatively small. In addition resonance shift data obtained in the autoclave could be compared with those obtained at 700 °C for a sample sealed in a quartz ampoule. This provided a means of correcting the thermocouple reading and fixing the Mo resistance thermometer calibration at the low-temperature end. The estimated error in sample temperature measurements at 700 °C is ± 10 °C.

The pressure medium employed was "prepurified" grade argon gas (99.995% purity). The gas was compressed to the working pressures by means of an electrically driven two-stage diaphragm compressor. Pressures were measured with a Bourdon manometer having a specified accuracy of ± 1 bar.

Most of the data below 700 °C were obtained with a ^{77}Se sample sealed under vacuum in a quartz ampoule (normal boiling point 685 °C). Thus the pressures for these measurements were simply the vapor pressures at the respective sample temperatures. In the early stages of these experiments, a sample of natural isotopic abundance (nominally 99.9999% purity) was also employed for low-temperature measurements at vapor pressure. The quartz ampoule runs were carried out using a conventional high-temperature NMR probe.[6] Sample temperatures were measured with a Pt–Pt 10 at.% Rh thermocouple in a reentrant well in the quartz cells such that the junction was in close thermal contact with the molten Se within.

Measurements were performed using pulsed NMR techniques, mainly at a frequency of 13.6 MHz. Additional data were obtained below 700 °C at 5.5 and 10.2 MHz. In the low-temperature range, signal-to-noise ratios were sufficiently high that data could be satisfactorily recorded using a boxcar integrator. Deterioration of the signal strengths at high temperature necessitated the use of a digital signal averager

(Nicolet Model 1072).

Resonance shifts were measured by sweeping the magnetic field through resonance while integrating the free-induction decay with the boxcar integrator.[7] The integrated output was either recorded directly with an XY recorder or stored in the memory of the signal averager if the signal-to-noise ratio required repetitive sweeps. The magnetic field was monitored at a point outside the autoclave by means of an auxiliary ^2H NMR in a D_2O sample. The absolute value of the field at the Se sample position was not determined; rather, the shift was defined to be zero for the liquid at the melting point and subsequent shifts were measured relative to this value.

Three different nuclear relaxation times were measured under various conditions. The spin-lattice relaxation time (T_1) was measured with a standard $\pi - \frac{1}{2}\pi$ sequence. The spin-spin or transverse relaxation time (T_2) was measured from the decay of the amplitude of the spin echo obtained with a $\frac{1}{2}\pi - \pi$ sequence. Finally, the spin-phase memory time (T_2^*) was determined from analysis of the free-induction decay following a single $\frac{1}{2}\pi$ pulse. The free-induction decays were exponential except below about 400 °C where magnetic field inhomogeneity affected the decay shapes.

The high cost of isotopically enriched ^{77}Se and the unavoidable loss of some material in the course of each high-pressure run imposed a limit on the total amount of data which could be acquired. The material losses in the autoclave occurred at the Ar-Se interface in the reservoir and through ruptures of the measurement cell at high temperatures in some runs. The experimental program was therefore designed with the aim of probing the most interesting regions of the P-T phase diagram within the limited number of experimental runs allowed. Pressures and temperatures were chosen so that all three regions of differing electronic behavior would be studied, i.e., the semiconducting, metallic, and insulating regions indicated in Fig. 1. The experimental program was begun with 4.0 g of enriched ^{77}Se and was terminated when roughly half this material remained. Some of the material "lost" in the autoclave was later recovered by distillation from the various internal components and by chemical treatment of the copper reservoir box.

III. EXPERIMENTAL RESULTS

A. Resonance shifts

The magnetic field value of the ^{77}Se NMR was measured as a function of pressure and temperature at a fixed frequency of 13.6 MHz. As molten Se was heated under its own vapor pressure, there developed a gradual shift relative to the resonant field at the melting point. The sign of the shift, down field from the reference point at T_m, indicated a paramagnetic enhancement of the local field at the ^{77}Se nucleus. We shall designate the fractional shift by $\Delta H/H$ defined according to $\Delta H/H \equiv [H(\text{reference}) - H(\text{resonance})]/H(\text{resonance})$. The shift continued to increase when the temperature was raised above 700 °C under approximately isobaric conditions. These shift data are shown as a function of temperature in Fig. 3. Comparison of the 100 and 400-bar isobars indicates a clear positive pressure coefficient for the shift in the range 800–1200 °C. The 400-bar isobar shows a maximum at about

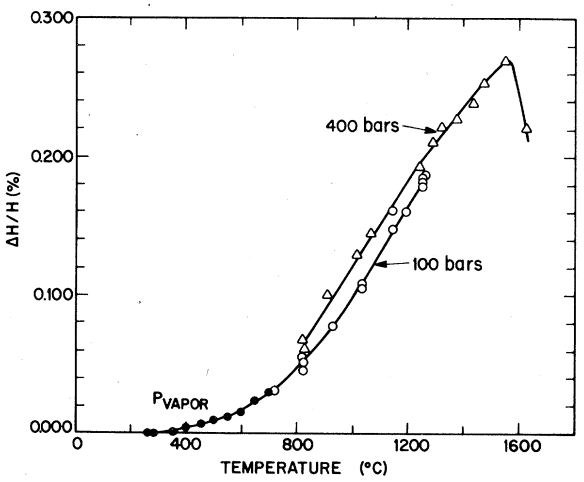

FIG. 3. ^{77}Se resonance shifts vs temperature for liquid selenium. Solid points denoted P_{VAPOR} obtained with samples sealed under vacuum in quartz ampoules. Data at 100 and 400 bars obtained using internally heated autoclave.

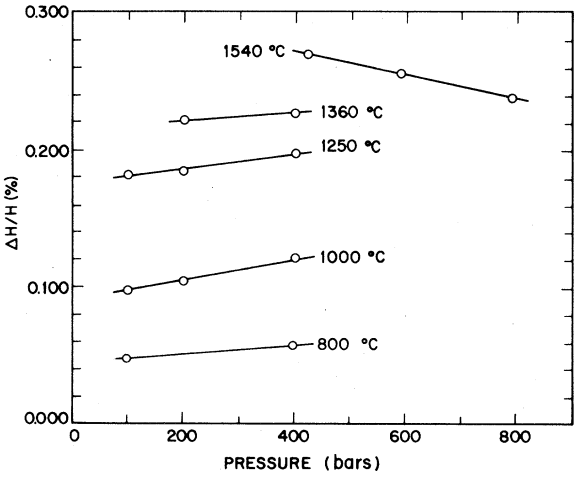

FIG. 4. ^{77}Se resonance shifts vs pressure at representative temperatures for liquid selenium.

1550 °C where the shift is $\Delta H/H = 0.270 \pm 0.005\%$.

The pressure dependence of the shift depends on temperature and, in fact, becomes negative above about 1400 °C. This is illustrated in Fig. 4 where the shift is plotted as a function of pressure for several representative temperatures. These isotherms were constructed from smoothed isobars such as those shown in Fig. 3

B. Relaxation rates

Nuclear relaxation rates $1/T_1$, $1/T_2$, and $1/T_2^*$ were measured from 193 °C where the liquid was supercooled up to 1435 °C at 410 bars. These data are presented in Fig. 5 where the rates are plotted in semilog form against $1/T$. Three temperature ranges of distinctly different relaxation characteristics are evident. We denote these by regions I, II, and III, respectively.

In region I ($T \lesssim 250$ °C), the spin-echo decay rate $1/T_2$ decreases with temperature while the spin-lattice relaxation rate $1/T_1$ increases. In this region, $1/T_1$ is weakly dependent on frequency over the range 5.5–13.6 MHz. This dependence tends to vanish as the temperature decreases into the supercooled liquid range. On the other hand, $1/T_2$ increases sharply with frequency at the lowest temperature attained. At 13.6 MHz and 193 °C, $1/T_2$ is 3.8 times the value measured at 5.5 MHz.

Between 250 and 700 °C (region II) both the spin-lattice and spin-spin relaxation rates increase sharply with temperature. This temperature dependence is approximately exponential in $1/T$. Above 400 °C, spin-spin relaxation rates were measured from the free-induction decay lifetime $1/T_2^*$ by subtracting from the latter a constant correction for magnetic field inhomogeneity. The corrected $1/T_2^*$ values join smoothly onto the spin-echo decay rates in the range 400–500°C. In region II, $1/T_2$ is independent of frequency whereas $1/T_1$ increases considerably with decreasing frequency. The ratio $(1/T_2)/(1/T_1)$ decreases as the temperature is raised until at 700 °C, $1/T_2$ and $1/T_1$ are nearly equal.

Preliminary relaxation rate measurements in region II were made with samples of natural isotopic abundance. The results for natural and enriched material were in fair agreement although $1/T_1$ was systematically higher for the natural Se by about 20%. Part of this discrepancy may be due to the poor signal-to-noise ratios obtained with natural Se. However, the result also suggests a systematic enhancement of $1/T_1$ due to impurities. In our experiments only the enriched material was distilled before use and we believe that these samples where chemically purer than the natural material.

Relaxation data have also been reported for regions I and II by Brown, Moore, and Seymour[8] (195–410 °C) and by Seymour and Brown[9] (160–370 °C). Enriched ^{77}Se was used in the latter study which yielded relaxation rates at 11 MHz which were about 20% higher than our own results interpolated between 10.2 and 13.6 MHz. However, the 7 MHz rates reported by those authors exceeded by nearly a factor of 2 the interpolation of our results between 5.5 and 10.2 MHz. The temperature dependences of the rates reported by Seymour and Brown are very similar to ours. These results reinforce our inference

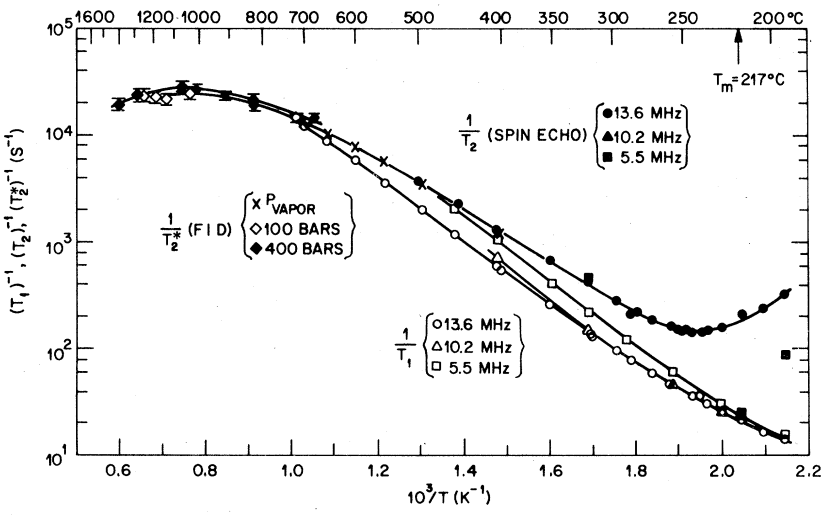

FIG. 5. Logarithm of the ^{77}Se nuclear relaxation rates vs $1/T$ for liquid selenium. $1/T_1$, spin-lattice relaxation rate; $1/T_2$, spin-spin relaxation rate measured from decay of spin-echo amplitude; $1/T_2^*$, spin-phase memory time measured from free-induction decay.

of an impurity-induced enhancement of $1/T_1$ which does not affect the temperature dependence.

Region III ($T \gtrsim 700\,°C$) is the range studied in the high-pressure autoclave. Here, $1/T_1$ and $1/T_2^*$ are presumed to be equal and only $1/T_2^*$ was measured. The relaxation rates exhibit a broad maximum at about 1000 °C. Data at 100 and 400 bars in the range 700–1250 °C exhibit a barely resolvable trend toward higher rates at the higher pressure.

IV. ANALYSIS AND INTERPRETATION

A. Structural and electronic properties of normal liquid Se

In order to provide a background for interpreting the NMR results, we briefly summarize the main structural and electronic properties of "normal" liquid Se, i.e., liquid Se below the normal boiling point. More complete reviews may be found in Refs. 10 and 11.

1. Liquid structure

It was long believed that near T_m liquid Se consists of a mixture of Se_8^R ring molecules and polymeric chains.[12] Recently, however, the evidence[13] for an appreciable concentration of rings has been questioned.[14] Whether or not rings are present, the chains have a major influence on the physical properties and, for example, are responsible for the extraordinary vicosity—about 25 P at T_m.[10,15] The average chain length at this temperature was calculated to be about 10^4 atoms by Eisenberg and Tobolsky[12] but the studies of Keezer and Bailey[16] indicate that the actual length may be in the range 10^5–10^6 atoms.

Detailed investigations of the liquid structure by x-ray and neutron diffraction confirm the predominant twofold coordination.[17–19] The near-neighbor distance (2.38 Å) (Ref. 19) is essentially the same as in the trigonal crystal and a first coordination number of two is obtained from the area under the first peak in the radial distribution function.[19] Moscinski, Renninger, and Averbach[17] found evidence of parallel correlation between chains near the melting point. Inelastic neutron scattering by Axmann *et al.*[20] showed that the bond stretching vibrational mode survives melting with little frequency shift. Recent inelastic light scattering experiments[21] in the supercooled liquid, however, exhibit considerable additional line broadening compared with the amorphous solid.

The structure of liquid Se is strongly affected by temperature changes, even well below the normal boiling point. The mean chain length decreases rapidly with increased temperature with the result that the viscosity at the boiling point is only about 1 cP, comparable with other elemental liquids.[10] The denser packing resulting from shorter chains is believed to be responsible for an anomalous reduction in the thermal expansion coefficient observed above 1000 °C in liquid Se (Ref. 22) and at somewhat lower temperatures in Se-Te alloys.[23,24] The temperature-dependent mean chain length was calculated from the theory of the ring-chain equilibrium by Eisenberg and Tobolsky[12] and, more recently, by Misawa and Suzuki.[25]

It is evident that a close relationship exists between liquid and amorphous Se (a-Se) formed by rapid cooling of the melt. Amorphous Se also contains polymeric chain molecules. Light scattering data, long accepted as evidence for a high ring concentration in a-Se have been shown by Lucovsky[14] and by Lucovsky and Galeener[26] to be compatible with a disordered chain model and a total absence of rings. The molecular composition of a-Se is strongly affected by the thermal history of the parent liquid,[27] a result which is not surprising in light of the strong temperature dependence of the liquid structure. The similarity of liquid and a-Se extends to the electronic properties as well, a point which we consider in more detail in the next section.

2. Electronic properties

The semiconducting characteristics of liquid Se near the melting point can be shown qualitatively from a bond orbital model to be a consequence of the predominant twofold bonding. The atomic configuration of Se is $4s^2 4p^4$. Of the six available valence electrons, only two actually occupy covalent bonding states. The two $4s$ electrons are sufficiently low in energy that they do not participate in bonding; two $4p$ electrons form covalent bonds, one to each neighbor on the chain or ring, and the remaining two enter nonbonding "lone pair" states. The lone pair states are the highest filled states and form the valence band while the empty p antibonding states form the conduction band. The energy levels obtained from this molecular picture correspond to the major features of the band structure of crystalline trigonal Se.[28–30] The same bands are evident in the calculated density of states of a-Se.[31]

The experimentally observed electrical properties near T_m are normally extrinsic. Doping is provided by impurities,[32] especially O_2.[33] As the temperature is raised, the electrical conductivity increases rapidly and becomes much less sensitive to impurity concentration. The temperature dependence is thermally activated over limited ranges but the activation energy (ΔE) tends toward larger values at higher temperatures. Below 500 °C, Gobrecht *et al.*[33] observed a variety of values of ΔE in the range 0.2–1.2 eV depending on O_2 content and the thermal history of the sample. Between 500 and 720 °C, an intrinsic activation energy of 1.25 ± 0.02 eV was observed

whereas a value of 2.0 ± 0.3 eV was obtained between 720 and 1000 °C. Hoshino *et al.*[3] observed $\Delta E \sim 1.8$ eV in the range 900–1100 °C and an increase to ~ 2.2 eV at higher temperatures. Both the magnitude of the conductivity and the activation energy are dependent on pressure.[2,3,34,35]

The magnetic properties of liquid Se offer a sensitive indication of the relationship between the atomic arrangement and electronic structure. Near T_m liquid Se,[36–38] like *a*-Se,[39] exhibits only a temperature-independent diamagnetic susceptibility. This absence of paramagnetism in disordered Se and other amorphous chalcogenide semiconductors was long considered paradoxical because these materials were expected to contain appreciable numbers of dangling bonds, each occupied by a single electron. A recent proposal by Anderson[40] provides the basis for an explanation. According to this model, structural relaxation produces an effective negative electron correlation energy which favors creation of charged doubly occupied and empty defect states at the expense of the neutral, paramagnetic singly occupied centers. Anderson's suggestion has been extended and developed explicitly in terms of simple chemical bond concepts by Street and Mott[41] and by Kastner, Adler, and Fritzsche.[42] In the notation of Ref. 42, the most stable defects are proposed to be the negative doubly occupied dangling bond, C_1^-, and the positive threefold coordinated site C_3^+. At higher energies, accessible by thermal excitation, there are the neutral threefold defect C_3^0 and the paramagnetic dangling bond C_1^0.

The magnetic properties of liquid Se change significantly on heating well above T_m. A temperature-dependent paramagnetic contribution to the susceptibility begins to be evident at about 300 °C.[36–38,43,44] At 240 °C, an electron-spin-resonance (ESR) signal has been observed.[45] The signal intensity increases markedly as the temperature is raised further although increasing linewidths eventually "wipe out" the resonance above 400 °C. The paramagnetic states responsible for the susceptibility and ESR have been widely interpreted as thermally excited neutral dangling bond states C_1^0 (Ref. 43) although neutral threefold sites C_3^0 cannot be excluded *a priori*. The magnitude of the paramagnetic susceptibility provides a means of determining the concentration of paramagnetic centers and, with certain assumptions, the average number of atoms per polymer molecule. The temperature dependence yields the energy required to break a chain and create a pair of paramagnetic states.[45]

B. Semiconducting polymer region

1. Resonance shift and magnetic susceptibility: Hyperfine coupling and concentration of spins

We assume in this analysis that the resonance shift which develops above about 400 °C is due to paramagnetic neutral dangling bonds (C_1^0 centers) at the ends of the polymeric chains. At the present time there is disagreement as to whether the C_1^0 center or the neutral threefold site C_3^0 lies lower in energy in *a*-Se. Street and Mott[41] suggested that the C_1^0 state has the lower energy while Kastner, Adler, and Fritzsche[42] favored the C_3^0 defect. The calculations of Vanderbilt and Joannopoulos[31] indicate a slight preference for the C_1^0 center. The implications of these results for liquid Se are not clear, since the contributions of configurational entropy play a greater role in the more mobile liquid structure.[46] In Sec. IV B *4* we present evidence based on our measured hyperfine couplings that the majority of magnetic states in the liquid polymer are the C_1^0 chain-end centers. The implications of a minority of C_3^0 states will be discussed shortly.

In terms of the molar paramagnetic susceptibility χ_m^p of the centers, the shift can be expressed

$$\Delta H/H = (N_0 \gamma_e \gamma_n \hbar^2)^{-1} \langle A \rangle \chi_m^p - \sigma_{\text{chem}} \ , \tag{1}$$

where N_0 is Avogadro's number, γ_e and γ_n are the electronic and nuclear gyromagnetic ratios, respectively, $\langle A \rangle$ is the average hyperfine coupling constant, and σ_{chem} is the chemical shift.[47] We shall refer to the first term on the right-hand side of Eq. (1) as the paramagnetic shift contribution $(\Delta H/H)_p$. By defining the shift such that $\Delta H/H = 0$ at T_m, we have effectively set $\sigma_{\text{chem}}(T_m) = 0$.

If we make the simple assumption that the hyperfine field takes a series of discrete values corresponding to the various neighbor shells of the paramagnetic center, the average hyperfine coupling may be written

$$\langle A \rangle = \sum_{i=0}^{n} n_i A_i \ , \tag{2}$$

where A_i is the hyperfine coupling for the ith neighbor shell and n_i is the number of Se atoms in that shell. The term $i = 0$ refers to the chain-end atom ($n_0 = 1$), $i = 1$ is the first neighbor in the chain ($n_1 = 1$), $i = 2$ might be the nearest atom on a neighboring chain or ring ($n_2 = 4$),[18] etc. The coupling A_i can be expected to decrease rapidly with increasing i. It is assumed in writing Eq. (2) that individual Se atoms exchange rapidly enough to average over all possible sites during a nuclear Larmor period $\omega_0^{-1} \sim 10^8$ s. Our relaxation rate analysis (Sec. IV B) shows that this is valid over the temperature range in which the shift is observed.

The Curie susceptibility of the C_1^0 centers is proportional to c_s, the number of spins per gram atom of Se. Thus,

$$\chi_m^p = \frac{c_s N_0 \gamma_e^2 \hbar^2 S(S+1)}{3kT} \ , \tag{3}$$

where S is the spin of the localized magnetic mo-

ment. Combining Eqs. (1) and (3) we have

$$\frac{\Delta H}{H} = c_s \langle A \rangle \left(\frac{\gamma_e}{\gamma_n} \right) \frac{S(S+1)}{3kT} - \sigma_{\text{chem}} \tag{4}$$

so that given $\langle A \rangle$ and σ_{chem}, c_s may be determined from measurements of $\Delta H/H$.

The average hyperfine coupling $\langle A \rangle$ can be obtained from a correlation of the temperature dependent shift and total susceptibility. We assume that χ_m consists of a diamagnetic term χ_m^D in addition to the paramagnetic contribution χ_m^P described by Eq. (3)

$$\chi_m = \chi_m^P + \chi_m^D \ . \tag{5}$$

Now, if σ_{chem} and χ_m^D are independent of temperature, a plot of $(\Delta H/H)$ against χ_m should yield a straight line with slope $(N_0 \gamma_e \gamma_n \hbar^2)^{-1} \langle A \rangle$, and with intercept χ_m at $(\Delta H/H) = 0$. Such a plot is shown in Fig. 6 where we have used the recent susceptibility data of Gardner and Cutler (315–900 °C) (Ref. 38) and those of Freyland and Cutler (650–1250 °C).[44] Above about 700 °C a linear correlation is obtained with the slope corresponding to (in ergs)

$$\langle A \rangle = (2.87 \pm 0.24) \times 10^{-18}$$

or in terms of a magnetic hyperfine field (in kOe/μ_B)

$$\langle H_{\text{hf}} \rangle = 267 \pm 23 \ .$$

The above value of $\langle A \rangle$ indicates that the sum in Eq. (2) is dominated by the leading (chain-end) term A_0. We note, first, that our result is intermediate between the hyperfine fields 50 kOe and ~5 MOe given by Bennett, Watson, and Carter[48] for single, unpaired 4*p* and 4*s* electrons, respectively. Thus our result is roughly what should be expected for a small 4*s* admixture in the predominant 4*p* character of the defect state. In contrast the experimental value is roughly an order of magnitude larger than the hyperfine fields observed for ^{77}Se nuclei which are near neighbors to the magnetic site in spinel ferromagnets such as $CuCr_2Se_4$ (Ref. 49) or $CdCr_2Se_4$.[50] Furthermore defect state calculations by Vanderbilt and Joannopoulos[31] and photoinduced ESR studies by Bishop, Strom, and Taylor[51] suggest that the C_1^0 center is highly localized on the chain-end atom. We are thus led to the important conclusion that *the nuclei experiencing a significant local hyperfine field from the C_1^0 center are predominantly those just at the chain ends.*

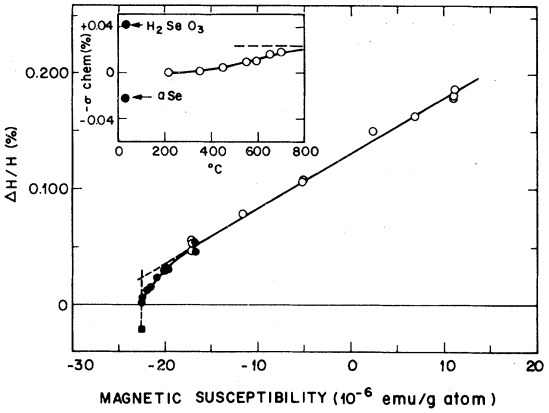

FIG. 6. ^{77}Se resonance shifts vs magnetic susceptibility for liquid selenium. Closed circles, susceptibility from Ref. 38; open circles, susceptibility from Ref. 44; closed square, shift from Ref. 76; susceptibility from Ref. 39 inset: apparent variation of chemical shift in nonlinear region of shift-susceptibility plot. Chemical shifts of *a*-Se and H_2SeO_3 are from Ref. 76.

TABLE I. Results of resonance shift analysis in polymer region. Concentrations of spins, c_s, from Eq. (4); spin densities, n_s, obtained using density data of Fischer (Ref. 22), extrapolated to temperatures above 1400 °C; maximum average number of atoms per polymer molecule, $\xi_{\max}$, from Eq. (8) with $f_r = 0$.

P (bars)	T (°C)	c_s	n_s (spin/cm^3)	$\xi_{\max}$
100	600	2.7×10^{-3}	7.3×10^{19}	750
100	800	1.5×10^{-2}	3.9×10^{20}	133
100	1000	5.5×10^{-2}	1.34×10^{21}	36
100	1200	1.21×10^{-1}	2.8×10^{21}	17
400	800	2.4×10^{-2}	6.3×10^{20}	84
400	1000	7.2×10^{-2}	1.78×10^{21}	28
400	1200	1.35×10^{-1}	3.2×10^{21}	15
400	1300	1.69×10^{-1}	3.9×10^{21}	12
400	1435	2.1×10^{-1}	4.7×10^{21}	10
400	1550	2.8×10^{-1}	6×10^{21}	7

Between T_m and 700 °C, the plot of $\Delta H/H$ vs χ_m is quite nonlinear and the slope increases sharply as the temperature decreases toward T_m. Even more striking is the observation of a sizable shift (0.022%) between the liquid at T_m and a-Se at room temperature, yet there is no detectable change in susceptibility over this interval. These features imply that χ_m^D is independent of temperature while σ_{chem} changes appreciably between room temperature and 700 °C. Taking the value of $\langle A \rangle$ determined above 700 °C we have extracted approximate values of the temperature-dependent chemical shift up to 700 °C. These results are shown in the inset of Fig. 6. It is interesting that these changes of σ_{chem} occur over the temperature range in which the ring concentration was reported to decrease markedly.[13] This suggests the possiblity that the effect is associated with different chemical shifts for the rings and chain polymer molecules. However, following the arguments of Lucovsky,[14] one could also explain this variation of σ_{chem} as a change in the relative concentrations of "ringlike" and "chainlike" dihedral angle sequences in a disordered chain.

Finally, we can use our values of $\langle A \rangle$ and σ_{chem} in Eq. (4) to determine c_s from the shift data. It is necessary to assume $S = \frac{1}{2}$ as expected for the single electron localized in a dangling bond. The resulting values of c_s are given in Table I together with the concentration of spin per unit volume, n_s, for representative temperatures in the polymer region.

2. *Temperature and pressure dependence of molecular structure*

We consider now the changes of molecular structure in the polymer region as the temperature and pressure are varied. These structural modifications are reflected in changes in the resonance shift as the number of paramagnetic chain ends varies.

The molecular structure of liquid Se is governed by the ring-chain equilibrium described by the reactions

$$\mathrm{Se}_8^R \overset{K_1}{\rightleftarrows} \mathrm{Se}_8 \ , \tag{6}$$

$$\mathrm{Se}_n \overset{K_2}{\rightleftarrows} \mathrm{Se}_{n-m} + \mathrm{Se}_m \ . \tag{7}$$

The initiation reaction (6) describes the opening of 8-membered rings (Se_8^R) to form linear diradicals (Se_8). The propagation reaction (7) describes the scission of an n-membered chain to form two shorter chains containing $n-m$ and m atoms, respectively. The equilibrium constant K_2 is assumed to be independent of n in this treatment.

Now in a simple linear-chain model without threefold coordinated sites, i.e., no branching, and only singly occupied C_1^0 chain ends, the average number of atoms per chain is

$$\xi = 2(1-f_r)/c_s \ , \tag{8}$$

where f_r is the fraction of Se atoms in ring molecules. If charged nonmagnetic centers C_3^+ and C_i^- are also present, it is easily shown that Eq. (8) still applies. If we define c_i to be the concentration of i-fold coordinated sites and $c_\pm$ to be the respective concentrations of C_3^+ and C_1^- centers, we have $c_1 = c_s + c_-$ and $c_3 = c_+ = c_-$. Thus $c_1 - c_3 = c_s$. But for a branched polymer molecule, the number of atoms is $\xi = 2/(c_1 - c_3)$ and, when the concentration of rings is taken into account, Eq. (8) follows immediately.

The possible presence of neutral threefold centers C_3^0 remains a complication to the use of Eq. (8). Using arguments similar to those of the preceding paragraph, it is easy to show that c_s in the denominator of Eq. (8) should be replaced by the difference $c_{s,1} - c_{s,3}$ of concentrations of C_1^0 and C_3^0 centers. If we measure the total concentration of spins $c_s = c_{s,1} + c_{s,3}$, then the error introduced by using Eq. (8) is such that we would overestimate ξ by a factor $(c_{s,1} - c_{s,3})/c_s$.

a. Temperature dependence. In principle, Eq. (8) can be used to obtain the average degree of polymerization ξ as a function of temperature from the values of c_s obtained from the resonance shifts. Unfortunately we have no independent measure of f_r over the range of our data. If we assume $f_r = 0$, Eq. (8) provides an upper limit on ξ. Briegleb's data,[13] while probably only of qualitative significance, indicate that $f_r \lesssim 0.15$ above 600 °C and that f_r decreases further with increasing temperature. Thus it is likely that the maximum values of ξ calculated from Eq. (8) are reasonably close to the actual values, and the difference should decrease at higher temperatures.

The experimental maximum values of ξ are given in Table I and are plotted against temperature in Fig. 7. The degree of polymerization obtained from NMR agrees well with the results of Massen, Weijts, and Poulis[43] obtained from magnetic susceptibility data at somewhat lower temperatures. All of the magnetic measurements are consistent with the results inferred for the melting-point region by Keezer and Bailey.[16] The chain lengths calculated by Eisenberg and Tobolsky are at least an order-of-magnitude shorter than these experimental results.

The temperature dependence of the paramagnetic contribution to the resonance shift provides a direct measure of the "enthalpy of scission," the energy required to break a chain. Following Koningsberger and de Neef[52] we write

$$M_0 = \frac{pK_2}{(1-p)^2} + 8p^8\frac{K_2}{K_1} \ , \tag{9}$$

where M_0 is the number of atoms present and p is the Flory parameter $\xi = (1-p)^{-1}$. Now for long chains ($\xi >> 1$) and negligible ring fractions ($K_1 >> 1$), it follows from Eq. (9) that

$$\xi = (M_0/K_2)^{1/2} = \exp(-\Delta S_{sc}/2R)\exp(\Delta H_{sc}/2RT) \ , \tag{10}$$

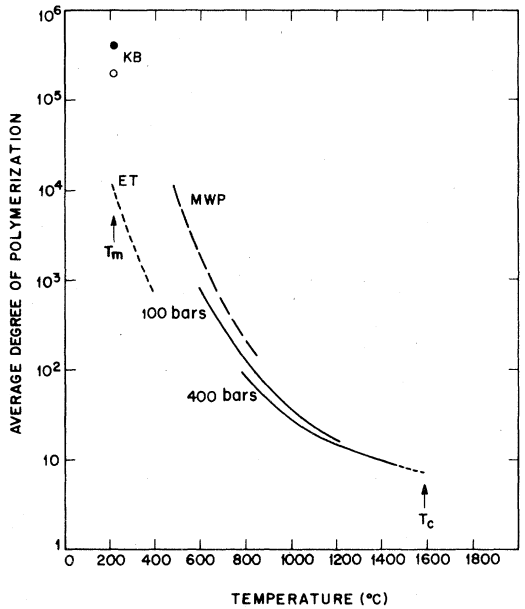

FIG. 7. Average degrees of polymerization (atoms per chain) vs temperature for liquid selenium. Full curves, ξ from resonance shift analysis and Eq. (8) assuming $f_r = 0$; dashed curve (MWP) ξ from magnetic susceptibility by Massen, Weijts, and Poulis, Ref. 43; broken curve (ET), ξ calculated from theory of ring-chain equilibrium by Eisenberg and Tobolsky, Ref. 12; circles (KB), results of Keezer and Bailey, Ref. 16, with and without the assumption of rings (solid and open circles, respectively).

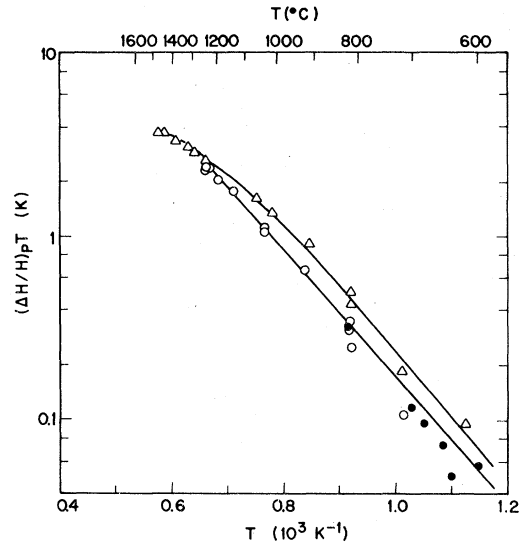

FIG. 8. Logarithm of the ^{77}Se paramagnetic resonance shift times absolute temperature vs $1/T$ for liquid selenium at various pressures. Closed circles, vapor pressure; open circles, 100 bars; open triangles, 400 bars.

where ΔS_{sc} and ΔH_{sc} are, respectively, the entropy and enthalpy of the scission reaction (7). Thus from Eqs. (4) and (8) with $f_r \ll 1$ we obtain for the paramagnetic shift

$$\left(\frac{\Delta H}{H}\right) = \langle A \rangle \left(\frac{\gamma_e}{\gamma_n}\right) \frac{S(S+1)}{3kT} \exp\left(\frac{\Delta S_{sc}}{2R}\right) \times \exp\left(\frac{-\Delta H_{sc}}{2RT}\right) . \quad (11)$$

If the entropy ΔS_{sc} is independent of temperature, a plot of $\ln[(\Delta H/H)_P T]$ against $1/T$ should exhibit slope $-\Delta H_{sc}/2R$. The factor $\frac{1}{2}$ in the arguments of the exponentials of Eq. (11) reflects the fact that a single scission event creates two chains and two new broken bonds.

A semilog plot of $(\Delta H/H)_P T$ against $1/T$ is shown in Fig. 8. The measured total shifts were corrected to obtain $(\Delta H/H)_P$ using chemical shifts inferred from the shift-susceptibility analysis of Fig. 6. The combined data for samples under vapor pressure and at 100 bars can be represented by an enthalpy of scission (in kcal/mole)

$$\Delta H_{sc} = 31.6 \pm 1.5$$

over the range 600–1250 °C. A slight tendency is observed for ΔH_{sc} (or possibly ΔS_{sc}) to decrease at higher temperatures. The 400-bar data are consistent with the 100-bar value of ΔH_{sc} in the range 600–900 °C but definitely exhibit a lower slope with further increase in temperature. The 100-bar and vapor-pressure values of ΔH_{sc} obtained from our NMR shifts agrees with value obtained from a corresponding analysis of the magnetic susceptibility by Gardner and Cutler (500–900 °C) (Ref. 38);

$$\Delta H_{sc} = 31.6 \pm 0.7$$

and by Freyland and Cutler (800–1250 °C),[44]

$$\Delta H_{sc} = 30.5 .$$

The latter authors also observed an increase in activation energy at lower temperatures. Finally, we note that our value of ΔH_{sc} agrees within experimental error with the result of Koningsberger *et al.* obtained from the temperature-dependent intensity of their ESR signal

$$\Delta H_{sc} = 29 \pm 3 .$$

b. Pressure dependence. Differentiation of the left-hand expression of Eq. (10) yields the pressure coefficient of the polymer size

$$\frac{d \ln \xi}{dP} = -\frac{1}{2} \frac{d \ln K_2}{dP} = \frac{\Delta V_2^{\ddagger}}{2RT} , \quad (12)$$

where we have introduced the activation volume $\Delta V_2^{\ddagger}$ associated with the equilibrium constant K_2. As in

TABLE II. Pressure dependence of resonance shift in polymer region. Pressure coefficient of shift, $d\ln(\Delta H/H)_P/dP$; activation volume per mole of polymer molecules for chain scission, $\Delta V_2^\dagger$; and volume per gram atom of Se, Ω_m.

T (°C)	$d\ln(\Delta H/H)_P/dP$ (10^{-4} bars^{-1})	$\Delta V_2^\dagger$ (cm^3/mole)	Ω_m (cm^3/g atom)[a]
800	10.2 ± 5.0	-180 ± 88	23.3
1000	8.9 ± 2.4	-186 ± 50	24.8
1250	3.3 ± 0.6	-83 ± 15	26.9
1360	1.4 ± 0.6	-38 ± 16	27.5

[a]Densities of Ref. 22.

the preceding discussion of the temperature dependence we consider only the temperature range in which the Se_8^R ring concentration is negligible. It then follows directly from Eqs. (4) and (8) that

$$\frac{d\ln(\Delta H/H)_P}{dP} = -\frac{\Delta V_2^\dagger}{2RT} \quad . \tag{13}$$

Values of $\Delta V_2^\dagger$ determined from the pressure dependence of the shift are presented in Table II. Also shown, for comparison, are the mean volumes per atom given by the density along the coexistence curve. It can be seen that the volume change on scission is relatively large, roughly 7 or 8 atomic volumes, in the low-temperature range where the chains are long. The activation volume decreases at higher temperatures and becomes comparable with the atomic volume in the range where the chains contain only a few atoms (Table I). The large negative activation volume for scission is qualitatively consistent with the observed thermal expansion anomaly[23,24] due to thermally activated scission at high temperatures.

3. *Relaxation of low temperatures: Molecular reorientation*

The minimum in the spin-spin relaxation rate ($^1/T_2$) at about 250 °C was observed previously by Seymour and Brown.[9] They suggested that the line broadening observed on cooling below 250 °C could be due to relaxation by the anisotropic chemical shift modulated by thermal reorientation of the polymer chain (and ring) molecules. The relaxation rates for this process can be expressed[53]

$$1/T_2 = \tfrac{1}{40}\gamma_n^2 H_0^2 \sigma_{z'}^2 (1+\tfrac{1}{3}\eta^2)[3\tilde{J}(\omega_0) + 4\tilde{J}(0)] \quad , \tag{14}$$

$$1/T_1 = \tfrac{6}{40}\gamma_n^2 H_0^2 \sigma_{z'}^2 (1+\tfrac{1}{3}\eta^2)\tilde{J}(\omega_0) \quad , \tag{15}$$

where $\sigma_{z'}$ is the principal component of the traceless part of the chemical shift tensor in the molecular coordinate frame, η is the asymmetry parameter, the reduced spectral density functions are given by

$$\tilde{J}(\omega) = \frac{2\tau_r}{1+\omega^2\tau_r^2} \quad , \tag{16}$$

and τ_r is the correlation time for molecular reorientation. For purposes of the present discussion we neglect differences in $\sigma_{z'}$, η, and τ_r due to the possible presence of both rings and chains and shall assume these to be represented by average quantities in Eqs. (14) and (15).

In the limit $\omega_0\tau_r >> 1$, Eqs. (14) and (15) reduce to the expressions

$$1/T_2 = \tfrac{1}{5}\omega_0^2\sigma_{z'}^2(1+\tfrac{1}{3}\eta^2)\tau_r \quad , \tag{17}$$

$$1/T_1 = \tfrac{6}{20}\sigma_{z'}^2(1+\tfrac{1}{3}\eta^2)\tau_r^{-1} \quad . \tag{18}$$

Thus, as τ_r becomes shorter on raising the temperature, $1/T_2$ should decrease; the frequency dependence should be $1/T_2 \propto \omega_0^2$. These qualitative features may be seen in the $1/T_2$ data below about 250 °C. At the lowest temperature, however, the ratio of $1/T_2$ values observed at 13.6 and 5.5 MHz (3.7 ± 0.3) is less than the predicted value $(13.6/5.5)^2 = 6.12$. This discrepancy disappears if the observed rates are corrected for a frequency-independent background by extrapolating the data obtained above 250 °C (Fig. 5). In this case the experimental ratio becomes 5.3 ± 1.0, in satisfactory agreement with Eq. (17).

Rotational correlation times τ_r can be obtained from $1/T_2$ data in the low-temperature range by means by Eq. (17) and chemical shift data. Since the molecular anisotropic chemical shift for the liquid is not known, we employ values of the anisotropic shift determined for crystalline trigonal Se by Koma and Tanaka.[54] The traceless part of the chemical shift tensor yields, on diagonalization, $\sigma_{z'} = 0.928 \times 10^{-4}$ and $\eta = 1$ whence

$$\sigma_{z'}^2(1+\tfrac{1}{3}\eta^2) = 1.148 \times 10^{-8} \quad .$$

Evaluation of Eq. (17) at 193 °C yields $\tau_r = 19.7 \pm 0.6$ μs. After correction for the frequency-independent

background, the analysis can be repeated at temperatures up to about 250 °C. The resulting values of τ_r are shown in the semilogarithmic plot given in Fig. 9. The rotational correlation time decreases rapidly between 193 and 250 °C and the temperature dependence can be represented by an activation energy of $\Delta E_r = 20.5 \pm 2.3$ kcal/mole over this range. The temperature dependence is similar to that of the viscosity which can be represented by $\Delta E_\eta = \cong 19$ kcal/mole over the range 220 to 250 °C.[10]

Rotational correlation times have been reported for the range 500 to 900 °C by Rasera and Gardner.[55] The data were obtained from the electric quadrupolar relaxation of excited ^{111}Cd nuclei in liquid Se measured by perturbed angular correlation (PAC). This correlation time (τ_{Cd}) was interpreted as the lifetime of a Cd-Se bond and is unlikely to be the same as the Se-Se bond rotation time which we have measured below 250 °C. In fact, a naive extrapolation of τ_r assuming $\tau_r \propto \eta^{-1}$ suggests that τ_r is roughly two orders of magnitude longer than τ_{Cd} in the 500–900 °C range.

Finally we point out that the spin-lattice relaxation observed near and below the melting point cannot be attributed to the anisotropic chemical shift mechanism. Although the rates become independent of frequency, as expected from Eq. (18), the observed rates are much too high for this process. For example, the value of τ_r deduced from $1/T_2$ at 193 °c implies $1/T_1 = 1.7 \times 10^{-4}$ s^{-1} from Eqs. (17) and (18).

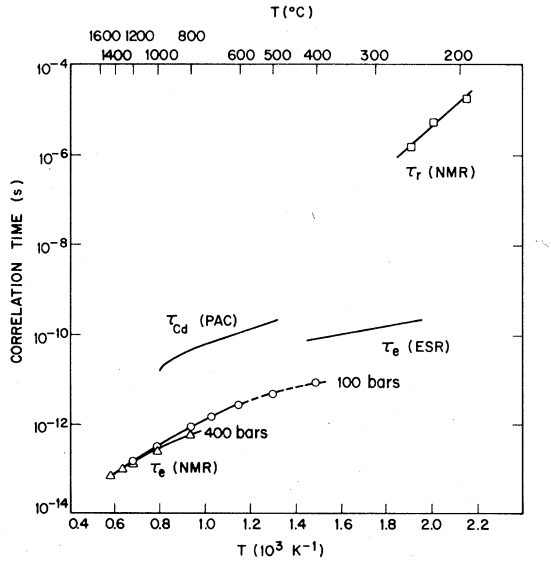

FIG. 9. Logarithm of correlation times in liquid selenium vs $1/T$. Open squares, molecular reorientation times from Eq. (17); open circles and triangles, hyperfine-field correlation times from Eq. (20) for 100 and 400 bars, respectively. PAC correlation time from Ref. 55; ESR spin-relaxation time from linewidths in Ref. 45.

The experimental result at this temperature is $1/T_1 = 13.9 \pm 0.4$ s^{-1}. Thus the observed relaxation is dominated by another process which is nearly independent of frequency at low temperatures and which increases strongly with temperature. This process is considered in detail in the next section.

4. *Relaxation by C_1^0 centers: Dynamics of localized spins*

It was first suggested by Brown, Moore, and Seymour[8] that localized electron spins at the chain ends could provide the dominant source of spin-lattice relaxation for ^{77}Se in the polymer region. The situation is analogous to proton relaxation in water containing paramagnetic ions such as Mn^{++}.[56] The coupling between the electron and nearby nuclei is assumed to be the isotropic scalar interaction of Eq. (2). This model leads to the standard theoretical expressions for the relaxation rates[57]

$$\frac{1}{T_1} = \tfrac{1}{3} S(S+1) c_s \left\langle \left[\frac{A}{\hbar} \right]^2 \right\rangle \frac{2\tau}{1+(\omega_s - \omega_0)^2 \tau^2} \quad , \tag{19}$$

$$\frac{1}{T_2} = \tfrac{1}{3} S(S+1) c_s \left\langle \left[\frac{A}{\hbar} \right]^2 \right\rangle \tau \left[1 + \frac{1}{1+(\omega_s - \omega_0)^2 \tau^2} \right] \quad , \tag{20}$$

where τ is the shorter of τ_a, the time of association of the electron and a particular nucleus, and τ_e the rate of fluctuation of the electron spin. The standard liquid state theory summarized by Eqs. (19) and (20) is valid as long as τ_a is sufficiently short that a nucleus cannot relax fully during a single encounter with a localized spin.

Several features of Eqs. (19) and (20) are of importance for interpreting nuclear relaxation in liquid Se. First, for correlation times sufficiently long that $(\omega_s - \omega_0)\tau \gtrsim 1$, $1/T_2$ is larger than $1/T_1$. It is easy to show from the ratio of Eqs. (19) and (20) that

$$\tau = [2(R-1)]^{1/2}/(\omega_s - \omega_0) \quad , \tag{21}$$

where $R \equiv (1/T_2)/(1/T_1)$. In the limit $(\omega_s - \omega_0)\tau >> 1$, $1/T_1 \propto (\omega_s - \omega_0)^{-2}$ and $1/T_2$ is independent of frequency. Finally, in the opposite limit where $(\omega_s - \omega_0)\tau << 1$, we have $1/T_1 = 1/T_2$ and both are independent of frequency. At a field such that the ^{77}Se frequency $\omega_0/2\pi$ is 13.6 MHz, the condition $(\omega_s - \omega_0)\tau = 1$ is satisfied for $\tau = 3.40$ ps. It is evident from the relaxation data shown in Fig. 5 that $(\omega_s - \omega_0)\tau << 1$ for temperatures above about 750 °C whereas the frequency dependence and unequal values of $1/T_2$ and $1/T_1$ indicate that $(\omega_s - \omega_0)\tau \gtrsim 1$ below about 600 °C.

As a test of the validity of the proposed model of relaxation by paramagnetic C_1^0 centers, we calculate

the magnitude of the relaxation rate using Eqs. (19) and (20). If we assume that the mean-square hyperfine coupling $\langle A^2 \rangle$ is equal to the square $\langle A \rangle^2$ of the coupling determined from the resonance shift analysis, the rate can be calculated with no adjustable parameters. At 600 °C we have from the shift analysis $c_s = 2.68 \times 10^{-3}$ and $\langle A \rangle = 2.87 \times 10^{-18}$ ergs. The ratio $R = (1/T_2)/(1/T_1) = 1.3\bar{4}$ substituted in Eq. (21) yields $\tau = 2.8$ ps. Evaluation of Eq. (19) using these parameters then yields in (s^{-1})

$$1/T_1 = 1.67 \times 10^3 \ ,$$

which is to be compared with the measured value at 600 °C

$$1/T_1 = 0.588 \pm 0.017 \times 10^3 \ .$$

Other potential relaxation processes such as nuclear dipole-dipole interactions or the anisotropic chemical shift are several orders of magnitude too weak to account for the observed relaxation. Thus, even though the theory overestimates the relaxation rate by nearly a factor of 3, the agreement is good enough to confirm that the proposed mechanism is correct.

The simplest explanation of the discrepancy between the observed and calculated values of T_1, is that there is a difference between the average hyperfine coupling $\langle A \rangle$ and the root-mean-square value $\langle A^2 \rangle^{1/2}$. The calculation at 600 °C requires $\langle A^2 \rangle^{1/2} = 0.59 \langle A \rangle$ in order to reconcile experiment and theory; essentially the same value is also obtained at 700 °C. The comparison cannot be made at higher temperatures because $R = 1$ and it is impossible to determine τ using Eq. (21). Nor can a comparison be made at temperatures below 600 °C, because a reliable value of c_s cannot be determined. Furthermore, as we shall discuss shortly, Eqs. (19) and (20) become invalid at lower temperatures.

It is easily seen from Eq. (2) that values of $\langle A^2 \rangle^{1/2}$ less than $\langle A \rangle$ might be expected if more than one nucleus experiences a significant hyperfine field from a given paramagnetic state. For example, if n nuclei experience equal local fields A_n, than $\langle A \rangle = nA_n$ and $\langle A^2 \rangle^{1/2} = n^{1/2} A_n$, i.e., $\langle A^2 \rangle^{1/2} = n^{-1/2} \langle A \rangle$. Now the calculations of Vanderbilt and Joannopoulos[31] indicate that the C_3^0 state is quite delocalized having no more than 15% of its amplitude on any one atom. If this is correct, we should expect $\langle A^2 \rangle^{1/2} / \langle A \rangle \leq 0.38$ for relaxation by C_3^0 centers. The observed value $\langle A^2 \rangle^{1/2} / \langle A \rangle = 0.59$ is clearly above this limit, but the result does admit the possibility that a minority of C_3^0 centers contribute to the relaxation.

In order to extract the temperature dependence of the correlation time over a wide range of temperatures, we have set $\langle A^2 \rangle^{1/2} = 0.59 \langle A \rangle$ as required to get consistency of the shifts and relaxation rates at 600 and 700 °C. We then use values of c_s obtained from the shift analysis to extract the correlation time from measured values of T_2 using Eq. (20). The analysis was extended from 600 down to 400 °C by extrapolating the exponential temperature dependence of $(\Delta H/H)_p T$ shown in Fig. 8. Values of τ for the range 400 to 1435 °C are shown in Fig. 9. The most important feature is that τ decreases strongly with increasing temperature, the variation amounting to about two orders of magnitude over this range. The temperature dependence cannot be described by a single thermal activation energy; the slope of the data in the semilog plot of Fig. 9 increases considerably at higher temperatures.

The hyperfine-field correlation times are at least two orders of magnitude shorter than the motional correlation times τ_{Cd} obtained by PAC studies. The rotational correlation times τ measured near and below T_m are even longer. These comparisons show that τ should be interpreted as τ_e, the electron-spin fluctuation time, rather than the nucleus-electron association time τ_a. However, τ_e is nearly an order of magnitude shorter than values of T_{2e} obtained from ESR linewidths (Fig. 9). This indicates that τ_e is the electron-electron exchange fluctuation time rather than the electron spin-lattice relaxation time which determines T_{2e}.

It is natural to expect the electron fluctuation times to become shorter due to stronger exchange interactions as the chains break and the concentration c_s increases. The relation of the correlation time to the spin density is seen clearly in Fig. 10 where $\log_{10} \tau_e$ is plotted against $n_s^{-1/3}$, the mean distance between paramagnetic centers. It is evident that τ_e decreases with increasing rapidity as $n_s^{-1/3}$ decreases. Moreover, the pressure dependence of τ_e seen in Fig. 9 is

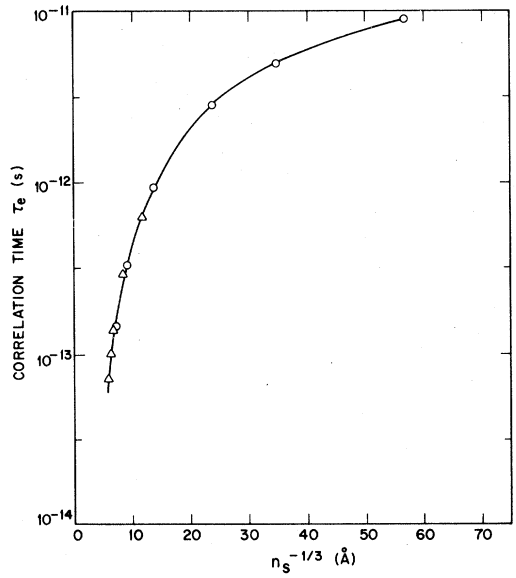

FIG. 10. ^{77}Se hyperfine-field correlation times vs (spin density)$^{1/3}$ at 100 (circles) and 400 bars (triangles).

no longer apparent indicating that τ_e is dependent only on $n_s^{-1/3}$ with no explicit temperature or pressure dependence. Extrapolation of the data in Fig. 10 suggests that metallic values of τ_e ($\sim 10^{-15}$ s) would be reached for values of $n_s^{-1/3} \sim 3$ Å, a reasonable value. The onset of metallic properties from the short-chain semiconducting polymer will be considered in the next section.

We turn now to the spin-lattice relaxation behavior observed in the low-temperature range of the polymeric semiconductor ($T \lesssim 400\,^\circ$C). We note first that the observed frequency dependence of $1/T_1$ is everywhere weaker than the ω_0^{-2} behavior predicted by Eq. (20) when $(\omega_s - \omega_0)\tau >> 1$. Furthermore as the temperature is lowered to the melting point and below, the frequency dependence gradually weakens until, at 193 °C, an essentially frequency-independent rate was observed. However, even in this range, the magnitude of the relaxation still far exceeds that expected for the nuclear dipole-dipole and anisotropic shift mechanisms. Because of the strength of the relaxation and the fact that the rates increase rapidly with temperature, we attribute the low-temperature relaxation to the same mechanism we have discussed for high temperatures, namely, interaction with paramagnetic C_1^0 centers.

The explanation for the loss of frequency dependence at low temperatures derives from the relatively long motional correlation times which occur when the chain polymers become very long. Recent investigations of nuclear relaxation of diffusing ions in superionic conductors containing paramagnetic impurities have demonstrated breakdown of Eqs. (19) and (20) when ions diffuse slowly enough to be fully relaxed during a single encounter with a paramagnetic center.[58,59] We should expect the same effect to occur in liquid Se when the association time τ_a is sufficiently long. Richards[59] has shown that Eqs. (19) and (20) are valid in the limit

$$y \equiv \tfrac{2}{3}\langle (A/\hbar)^2 \rangle S(S+1)\tau_e \tau_a << 1 \quad . \tag{22}$$

Whereas in the opposite limit, $y >> 1$, one obtains a frequency-independent rate

$$\frac{1}{T_1} = \frac{1}{T_2} = \frac{c_s}{\tau_a} \quad . \tag{23}$$

At the melting point of Se, extrapolation of the high temperature τ_e results yields $\tau_e \sim 3 \times 10^{-11}$; the rotational correlation times τ_r and extrapolated PAC τ_{Cd} results imply $10^{-9} < \tau_a < 10^{-7}$ s (Fig. 9). For a very rough estimate we take $\tau_a \sim 10^{-8}$ s and $\langle (A/\hbar)^2 \rangle = 2.6 \times 10^{18}$ rads^{-2} as before. These parameters correspond to $y \approx 0.4$. Thus the condition $y \sim 1$ occurs near or somewhat below the melting point which is consistent with the disappearance of the frequency dependence of $1/T_1$ in this temperature range. Because of the intervention of the anisotropic chemical shift relaxation, the expected equality of $1/T_1$ and $1/T_2$ is not observed. Finally, a rough estimate of the magnitude of $1/T_1$ from Eq. (23) is consistent with the measured rates. Straightforward extrapolation of the data in Table I according to $c_s \propto \exp(-\Delta H_{sc}/2RT)$ yields $c_s \sim 10^{-6}$ near T_m. Thus, for $\tau_a \sim 10^{-8}$ s, we estimate $1/T_1 = 1/T_2 = 10^2$ s^{-1} which is the correct order of magnitude. Of course we should not expect the limiting expression to hold exactly for $y \sim 1$, but this comparison demonstrates that the paramagnetic centers are responsible for spin-lattice relaxation throughout the liquid range.

C. Transition to the metallic state

1. Delocalization: Onset of Pauli susceptibility

Metallic conductivity values are obtained in fluid Se by application of pressure in the temperature range 1500–1600 °C (Fig. 1).[2,3,34,35] Before we discuss the onset of metallic properties, let us consider the state of the system at the limit of the semiconducting range. At 1550 °C and 400 bars the conductivity σ is about 20 $(\Omega\ \text{cm})^{-1}$ and the resonance shift is $\Delta H/H = 0.272\%$. Extension of the analysis of the preceding section yields $\xi \sim 7$ for the mean polymer size, $n_s \sim 6 \times 10^{21}$ spins/cm^3 and $n_s^{-1/3} \sim 5.5$ Å. Thus the localized model indicates that Se is a highly concentrated paramagnet under these conditions.

When pressure is applied at 1550 °C there is a sharp increase in conductivity accompanied by a decrease in shift. At the maximum pressure reached (790 bars) the conductivity is about 100 $(\Omega\ \text{cm})^{-1}$ and the shift is reduced by about 15% of its value at 400 bars. The reduction of shift can be explained in terms of the conversion from the Curie susceptibility of the localized C_1^0 centers to the Pauli susceptibility of extended states. For example, the Curie susceptibility χ_m^c of 6×10^{21} spins at 1550 °C is 55×10^{-6} emu/g atom; the Pauli susceptibility of the same number of free electrons, enhanced by electron-electron interactions, is about 25×10^{-6} emu/g atom. Thus, while the density of states created by delocalization of the dangling bond electrons is very likely to differ from the free-electron value, this simple comparison shows that a substantial reduction of susceptibility can be anticipated with delocalization.

An alternative approach is to consider the shift that might be expected in metallic Se at higher conductivities than could be reached in this experiment. The shift associated with the Pauli susceptibility in a fully degenerate metal is, of course, the Knight shift

$$K \equiv \Delta H/H = \tfrac{8}{3}\pi \langle |\Psi(0)|^2 \rangle_F \chi_a^P \quad , \tag{24}$$

where $\langle |\Psi(0)|^2 \rangle_F$ is the probability amplitude of the

conduction electrons averaged over all states within kT of the Fermi level and χ_a^P is the Pauli susceptibility per atom. Now a useful structural model for metallic Se is provided by liquid Te in the normal liquid range. It is believed that Te contains a large number of threefold coordinated sites[60–62] and such a structure can be easily imagined to evolve the polymeric Se structure after a high degree of chain rupture and branching has occurred. Evidence that this is the case is provided by studies of Se-Te alloys at high temperature and pressure. It was found that there is a qualitative equivalence of the effects of increased pressure and increased Te content.[63,64] Thus, since metallic conductivities are relatively weakly dependent on temperature, we can obtain a rough estimate of the susceptibility of metallic Se from the susceptibility of Te at the same value of conductivity. In the same way, the Knight shift of Se can be estimated from the shift data for liquid Te,[65] provided that we account for the increase in s-electron hyperfine-coupling strength $|\Psi(0)|^2$ associated with the higher atomic number of Te. A straightforward way to do this is to scale the Te shifts by the ratio of atomic hyperfine coupling for the two elements. Thus, we might expect

$$K(\mathrm{Se}) = K(\mathrm{Te}) \frac{|\Psi(0)|^2_{\mathrm{Se}}}{|\Psi(0)|^2_{\mathrm{Te}}} , \tag{25}$$

where the shifts are taken for the same conductivity σ.

The above approach is illustrated in Fig. 11 where we have plotted $\Delta H/H$ vs $\ln\sigma$ for Se along the 400 isobar and along the approximate isotherm at 1540 °C. The Knight shift of Se estimated according to Eq. (25) is also shown. The tendency for the shift to increase with increasing conductivity begins to break down when $\sigma \sim 50$ $(\Omega\,\mathrm{cm})^{-1}$ and is completely reversed along the 1540 °C isotherm. Extrapolation to higher conductivities suggests that the expected metallic shifts would be observed for $\sigma \sim 1000$ $(\Omega\,\mathrm{cm})^{-1}$. These estimated metallic shifts are substantially smaller than the shifts at lower conductivities, in agreement with our earlier estimates of the absolute values of the Curie and Pauli susceptibility.

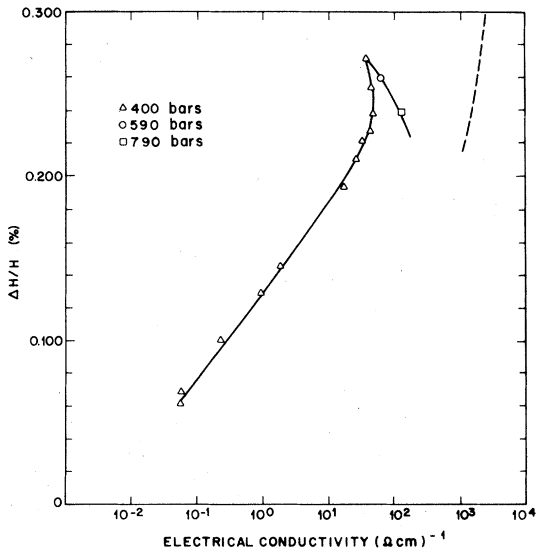

FIG. 11. ^{77}Se resonance shifts vs dc electrical conductivity for liquid selenium. Conductivity data from Refs. 2, 3, and 75. Dashed curve, estimated Knight shift for metallic selenium obtained by scaling ^{77}Te shift data for liquid tellurium (Ref. 65).

2. *Simple band model of the metal-nonmetal transition in Se*

The NMR data provide the basis for a qualitative band picture of the metal-nonmetal transition in expanded fluid Se. In order that the model be valid over a wide range of temperature and pressure, its most essential feature is the radical modification of the spectrum of electronic states caused by the structural transformations of the liquid. A rigid-band approach, while perhaps valid for the polymer at low temperatures, cannot be expected to apply in the presence of destruction of the chain structure and introduction of large numbers of threefold coordinated sites at very high temperatures.

A plausible scenario for development of the metallic state is illustrated by the sequence of densities of states shown in Fig. 12. For the low-temperature polymer [Fig. 12(a)] the molecular bond picture yields two filled bands, the p-bonding and nonbonding (lone pair) bands, and an empty p-antibonding conduction band. The work of Vanderbilt and Joannopoulos[31] shows that neutral dangling bonds introduce a narrow band of defect states in the center of the gap. On heating, the number of gap states grows [Fig. 12(b)] at the expense of states in the valence and conduction bands. The latter can be expected to broaden as the short-range order of the long polymeric chains is destroyed. Preservation of the Curie-like susceptibility shows that the band of defect states remains narrower than $\sim kT$ up to 1550 °C and 400 bars ($kT \sim 0.16$ eV). It is at this point that application of pressure leads to rapid delocalization of the gap states [Fig. 12(c)] to form a pseudogap of either weakly localized or strongly scattering extended states. Delocalization is a consequence of structural collapse in which localized C_1^0 states are destroyed in favor of delocalized threefold sites

$$C_2^0 + C_1^0 \rightarrow C_3^0 .$$

The conductivity at delocalization is on the order of 100 $(\Omega\,\mathrm{cm})^{-1}$ which is comparable with the minimum metallic conductivity proposed by Mott.[66] Fi-

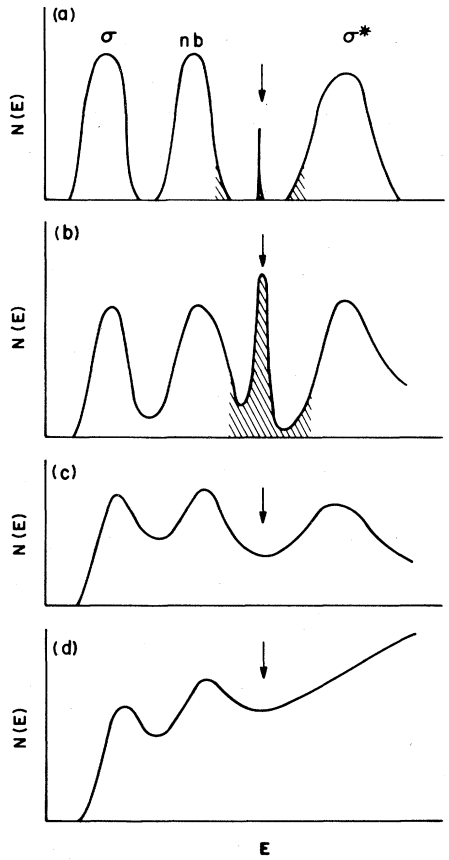

FIG. 12. Suggested development of density of states $N(E)$ vs energy E through metal-nonmetal transition in expanded liquid selenium: (a) polymer region near T_m; σ and σ^* are p-bonding and antibonding bands, respectively. nb denotes nonbonding (lone pair) valence band. States near Fermi energy (arrow) are localized chain-end states (C_1^0). Shading at band edges denotes states localized by disorder. (b) Limit of polymer region near 1550 °C and 400 bars. Gap contains narrow band of localized C_1^0 states. (c) Delocalization of C_1^0 under pressure at high temperature to form pseudogap. (d) Metallic state of fluid selenium.

nally, application of additional pressure [Fig. 12(d)] yields an essentially metallic band similar to that of liquid Te.

3. *Comparison of Se with chalcogen alloys*

A number of binary metal-chalcogen liquid alloys exhibit metal-nonmetal transitions that are superficially similar to that of expanded Se.[10,67] The binary alloys generally exhibit nonmetallic electronic properties near the melting point of a simple stoichiometric composition (e.g., Ga_2Te_3). At high temperatures, or for compositions rich in either component, the liquids are metallic. However, the NMR data show that there are basic differences in the nature of electron localization in the two cases. In the alloys, the Knight shift tends monotonically to zero as the conductivity decreases.[68–70] This has been interpreted as due to development of a progressively deeper pseudogap. Strong enhancement of the Korringa relaxation rate shows that the states in the deepening pseudogap become progressively more localized.[68–71] However, in the alloys there is never observed the appearance of a Curie susceptibility and correspondingly large shift as is the case for Se. Thus whereas in Se, localization is manifest in the development of a narrow band of strongly localized gap states, the states in the pseudogap of the alloys occupy a range of energies which is considerably broader than kT, on the order of the gap width. The explanation of this difference in behavior in terms of the chemical bonding and local atomic order in the two cases poses an interesting challenge for theory.

D. Transition to the insulating state

In the vicinity of the liquid-gas critical point, Se is an insulator with conductivity less than 0.1 $(\Omega\ \text{cm})^{-1}$.[2,3] Beginning from the upper limit of the semiconducting polymer (~ 1550 °C and 400 bars), the conductivity drops sharply due, presumably, to the rapid reduction in the density as the critical region is approached. By extrapolation of the known temperature-dependent composition of Se vapor at lower temperatures[72] and by comparison with the optical properties of supercritical S vapor,[73] it can be inferred that supercritical Se consists mainly of molecular Se_2 with smaller concentrations of atomic Se and other small molecules up to Se_8^R. Thus the semiconductor to insulator transition is associated with the structural change from short linear diradicals to various smaller species at lower densities.

In distinct contrast with the electrical conductivity, the magnetic properties of Se are not strongly affected by the transition to the insulating vapor. In particular, only a modest reduction in shift is observed between 1550 and 1625 °C at 400 bars, even though the conductivity drops by several orders of magnitude. Thus the supercritical vapor retains a relatively large paramagnetism.

It was emphasized by Freyland and Cutler[44] that, contrary to the tentative conclusion of Massen *et al.*,[43] the ground state of molecular Se_2 is known to be a singlet.[74] Thus, unlike S_2 and O_2 whose ground states are triplets, Se_2 should exhibit no paramagnetism in the ground state. At high temperatures, there are two reasons to expect increased paramagnetism. First, the magnetic triplet state of Se_2 can be thermally excited: Meschi and Searcy[74] estimate that roughly 20% of the Se_2 should be in the triplet state at 2000 K. Second there should be appreciable amounts of atomic Se due to thermal dissociation of Se_2. Frey-

land and Cutler have proposed atomic Se as the source of the paramagnetism of Se vapor between 1090 and 1200 °C.[44]

The magnitude of the NMR shift at 1625 °C is consistent with reasonable amounts of either triplet Se_2 or atomic Se. If we take $A \sim 1 \times 10^{-18}$ ergs for a rough estimate, the experimental shift value substituted in Eq. (1) yields $\chi_m^p \sim 100 \times 10^{-6}$ emu/g atom. This susceptibility corresponds to roughly 40% of the atoms being in the form of triplet Se_2 or, alternatively, some 13% in the $^3P_2$ atomic ground state. Although 40% is somewhat high for the triplet Se_2 fraction given the triplet-singlet splitting of 0.36 eV, the large uncertainty in hyperfine coupling A makes it impossible to draw a firm conclusion regarding the species responsible for paramagnetism at 1625 °C.

The most surprising feature of the susceptibility is its apparently weak temperature dependence. Freyland and Cutler[44] observed values in the range 74–85 emu/g atom between 1090 and 1200 °C with no discernible trend with temperature. Our estimate indicates, further, that χ_m changes by less than about a factor of 2 up to 1625 °C. This result is unexpected for either Se_2 or atomic Se since triplet excitation and molecular dissociation should both exhibit strong temperature dependences.

V. SUMMARY AND CONCLUSIONS

The NMR investigation described in this paper has yielded considerable new information about the structural changes and associated electronic effects in liquid Se. In the polymer region we have attributed the observed shift and relaxation process to the effects of localized paramagnetic defects—the neutral chain-end dangling bond C_1^0. Analysis of the temperature and pressure dependence of the shift yielded the hyperfine coupling, the enthalpy of chain scission, the temperature-dependent concentrations of spins and inferred average polymer sizes, and the activation volume for pressure-induced chain scission.

Spin-spin relaxation rates yielded the correlation times for molecular rotation near the melting point and in the supercooled liquid. This time is about 10^{-5} s at the melting point and it decreases rapidly with increasing temperature. Relaxation rates above 400 °C yielded the correlation times for fluctuation of the localized moment of the C_1^0 defect. These times decrease with temperature from about 10^{-11} s at 400 °C to less than 10^{-13} s above 1400 °C. We attribute this effect to increased exchange interactions among the localized spins as their concentration increases.

At roughly 1550 °C and 400 bars, the liquid reaches a special condition which we have called the limit of the semiconducting polymer region. At this point, a large shift indicates that the liquid is a nonmetallic concentrated paramagnet. The average polymer molecule contains about 7 atoms and the spin-fluctuation time due to exchange is $\sim 5 \times 10^{-14}$ s. Further heating leads to the insulating, paramagnetic supercritical fluid. Application of pressure at the polymer limit produces a sharp change in the magnetic properties as the paramagnetic centers delocalize and a metallic state ensues.

Delocalization of the defect states coincides with the electrical conductivity reaching the minimum metallic conductivity of Mott. The behavior of Se at the metal-nonmetal transition contrasts with that of binary chalcogen alloys which do not show a large Curie-like susceptibility or shift below the minimum metallic conductivity. This result implies that the localized states in the pseudogap of the alloys do not represent well characterized defects as in Se, but may be much more weakly localized, extending over several atoms.

The paramagnetic susceptibility of the supercritical insulating vapor is consistent with the presence of either atomic Se in the $^3P_2$ ground state or excited triplet Se_2. However, the temperature dependence of the susceptibility, inferred by comparison with vapor susceptibilities at lower temperatures is surprisingly weak for either of these species. The magnetic properties and molecular composition of dense Se vapor clearly require further investigation.

ACKNOWLEDGMENTS

We wish to express our appreciation to F. Hensel, H. Hoshino, and R. W. Schmutzler for numerous helpful discussions of the experimental aspects and interpretation of these experiments. M. Cutler, W. Freyland, and J. A. Gardner kindly provided us with their susceptibility data prior to publication and contributed to our work through several stimulating discussions. U. El-Hanany generously helped out during one of the more strenuous experimental runs and A. Kornblit carried out a computer-assisted analysis of some of the data. G. F. Brennert provided valuable technical assistance throughout the experimental program.

[1]M. Edeling, R. W. Schmutzler, and F. Hensel, Philos. Mag. B 39, 547 (1979).
[2]H. Hoshino, R. W. Schmutzler, and F. Hensel, Ber. Bunsenges. Phys. Chem. 80, 27 (1976).
[3]H. Hoshino, R. W. Schmutzler, W. W. Warren, and F. Hensel, Philos. Mag. 33, 255 (1976).
[4]Substrate glaze No. 01328-C, Owens-Illinois, Inc., P. O. Box 1035, Toledo, Ohio 43666.
[5]Oak Ridge National Laboratory, Isotope Sales, P. O. Box X, Oak Ridge, Tennessee 37830.
[6]See, for example, U. El-Hanany and W. W. Warren, Jr., Phys. Rev. B 12, 861 (1975).
[7]W. G. Clark, Rev. Sci. Instrum. 35, 316 (1964).
[8]D. Brown, D. S. Moore, and E. F. W. Seymour, J. Non-Cryst. Solids 8–10, 256 (1972).
[9]E. F. W. Seymour and D. Brown, in *Properties of Liquid Metals,* edited by S. Takeuchi (Taylor and Francis, London, 1973), p. 399.
[10]V. M. Glazov, S. N. Chizhevskaya, and N. N. Glagoleva, *Liquid Semiconductors* (Plenum, New York, 1969), p. 84.
[11]W. C. Cooper and R. A. Westbury, in *Selenium,* edited by R. A. Zingaro and W. C. Cooper (Van Nostrand, New York, 1974), Chap. 3.
[12]A. Eisenberg and A. V. Tobolsky, J. Polym. Sci. 46, 19 (1960).
[13]G. Briegleb, Z. Phys. Chem. Abt. A 144, 321 (1929).
[14]G. Lucovsky, in *Selenium and Tellurium,* edited by E. Gerlach and P. Grosse (Springer, Berlin, 1979).
[15]S. Dobinski and J. Wesolowski, Bull. Acad. Pol. A 9 (1937).
[16]R. C. Keezer and M. V. Bailey, Mater. Res. Bull. 2, 185 (1967).
[17]J. Moscinski, A. Renninger, and B. L. Averbach, Phys. Lett. A 42, 453 (1973).
[18]G. Tourand, J. Phys. (Paris) 34, 937 (1973).
[19]M. Misawa and K. Suzuki, Trans. Jpn. Inst. Met. 18, 427 (1977).
[20]A. Axmann, W. Gissler, A. Kollmar, and T. Springer, Discuss. Faraday Soc. 50, 74 (1970).
[21]P. J. Carroll and J. S. Lannin, in *Proceedings of the Eighth International Conference on Amorphous and Liquid Semiconductors, Cambridge, Mass., 1979,* edited by W. Paul and M. Kastner (North-Holland, Amsterdam, 1980), p. 1277.
[22]R. Fischer, dissertation (University of Marburg, 1978) (unpublished).
[23]J. Ruska, in *Amorphous and Liquid Semiconductors,* edited by J. Stuke and W. Brenig (Taylor and Francis, London, 1974), p. 779.
[24]H. Thurn and J. Ruska, J. Non-Cryst. Solids 22, 331 (1976).
[25]M. Misawa and K. Suzuki, J. Phys. Soc. Jpn. 44, 1612 (1978).
[26]G. Lucovsky and F. L. Galeener, in *Proceedings of the Eighth International Conference on Amorphous and Liquid Semiconductors, Cambridge, Mass., 1979,* edited by W. Paul and M. Kastner (North-Holland, Amsterdam, 1980), p. 1209.
[27]A. I. Popov, J. Phys. C 9, 675 (1976).
[28]J. Treusch and R. Sandrock, Phys. Status Solidi 16, 487 (1966).
[29]R. Sandrock, Phys. Rev. 169, 642 (1968).
[30]H. Wendel, R. M. Martin, and D. J. Chadi, Phys. Rev. Lett. 38, 656 (1977).
[31]D. Vanderbilt and J. D. Joannopoulos, Phys. Rev. Lett. 42, 1012 (1979).
[32]D. Sh. Abdinov, S. I. Mekhtieva, E. G. Akhundova, and V. R. Namazov, Russ. J. Phys. Chem. 47, 827 (1973).
[33]H. Gobrecht, D. Gawlik, and F. Mahdjuri, Phys. Kondens. Mater. 13, 156 (1971).
[34]V. A. Alekseev, V. G. Ovcharenko, Yu. F. Ryshkov, and M. V. Sadovskii, JETP Lett. 24, 189 (1977).
[35]V. A. Alekseev, V. G. Ovcharenko, Yu. F. Ryshkov, and A. A. Andreev, in *Proceedings of the Sixth International Conference on Amorphous and Liquid Semiconductors, Leningrad, 1975* (Academy of Sciences, Moscow, 1976), Vol. 2, p. 395.
[36]G. Busch and O. Vogt, Helv. Phys. Acta 30, 224 (1957).
[37]M. Risi and S. Yuan, Helv. Phys. Acta 33, 1002 (1960).
[38]J. A. Gardner and M. Cutler, Phys. Rev. B 20, 529 (1979).
[39]B. G. Bagley, F. J. DiSalvo, and J. V. Waszczak, Solid State Commun. 11, 89 (1972).
[40]P. W. Anderson, Phys. Rev. Lett. 34, 953 (1975).
[41]R. A. Street and N. F. Mott, Phys. Rev. Lett. 35, 1293 (1975).
[42]M. Kastner, D. Adler, and H. Fritzsche, Phys. Rev. Lett. 37, 1504 (1976).
[43]C. H. Massen, A. G. L. M. Weijts, and J. A. Poulis, Trans. Faraday Soc. 60, 317 (1964).
[44]W. Freyland and M. Cutler (unpublished).
[45]D. C. Koningsberger, J. H. M. C. van Wolput, and P. C. U. Rieter, Chem. Phys. Lett. 8, 145 (1971).
[46]M. Cutler, in *Amorphous and Liquid Semiconductors,* edited by W. E. Spear (Center for Industrial Consultancy and Liason, Edinburgh, 1977), p. 833.
[47]In contrast with the definition of $\Delta H/H$ given in Sec. III A, the chemical shift is conventionally defined as $\sigma_{\text{chem}} = [H(\text{resonance}) - H(\text{reference})]/H(\text{reference})$. Thus for $\sigma_{\text{chem}} << 1$, the paramagnetic shift contribution in Eq. (1) is $(-\sigma_{\text{chem}})$.
[48]L. H. Bennett, R. E. Watson, and G. C. Carter, in *Electronic Density of States,* edited by L. H. Bennett (National Bureau of Standards, Washington, D. C., 1971), Special Publ. 323, p. 601.
[49]M. Yokoyama, R. Watanabe, and S. Chiba, J. Phys. Soc. Jpn. 23, 450 (1967).
[50]S. B. Berger, J. I. Budnick, and T. J. Burch, Phys. Rev. 179, 272 (1969).
[51]S. G. Bishop, U. Strom, and P. C. Taylor, Phys. Rev. B 15, 2278 (1977).
[52]D. C. Koningsberger and T. de Neff, Chem. Phys. Lett. 14, 453 (1972).
[53]A. Abragam, *Principles of Nuclear Magnetism* (Oxford, London, 1961), p. 315.
[54]A. Koma and S. Tanaka, Solid State Commun. 10, 823 (1972).
[55]R. L. Rasera and J. Gardner, Phys. Rev. B 18, 6856 (1979).
[56]N. Bloembergen, J. Chem Phys. 27, 572 (1957).
[57]A. Abragam, *Principles of Nuclear Magnetism* (Oxford, London, 1961), p. 306.
[58]R. D. Hogg, S. P. Vernon, and V. Jaccarino, Phys. Rev. Lett. 39, 481 (1977).
[59]P. M. Richards, Phys. Rev. B 18, 6358 (1978).
[60]B. Cabane and J. Friedel, J. Phys. (Paris) 32, 73 (1971).
[61]G. Tourand, Phys. Lett. A 54, 209 (1975).
[62]J. F. Enderby and M. Gay, in *Proceedings of the Eighth International Conference on Amorphous and Liquid Semiconductors, Cambridge, Mass., 1979,* edited by W. Paul and M. Kastner (North-Holland, Amsterdam, 1980), p. 1269.

[63]A. A. Andreev, V. A. Alekseev, A. L. Manukyan, and L. N. Shumilova, Sov. Phys. Solid State 15, 277 (1973).
[64]H. Endo, H. Hoshino, R. W. Schmutzler, and F. Hensel, in *Liquid Metals, 1976,* edited by R. Evans and D. A. Greenwood (Institute of Physics, Bristol, 1977), p. 412.
[65]W. W. Warren, Jr., Phys. Rev. B 6, 2522 (1972).
[66]N. F. Mott, Philos. Mag. 19, 835 (1969).
[67]M. Cutler, *Liquid Semiconductors* (Academic, New York, 1977), Chaps. 7 and 8.
[68]W. W. Warren, Jr., Phys. Rev. B 3, 3708 (1971).
[69]W. W. Warren, Jr., Non-Cryst. Solids 8–10, 241 (1972).
[70]W. W. Warren, Jr., in *Liquid Metals, 1976,* edited by R. Evans and D. A. Greenwood (Institute of Physics, Bristol, 1977), p. 436.
[71]W. W. Warren, Jr., and G. F. Brennert, in *Amorphous and Liquid Semiconductors,* edited by J. Stuke and W. Brenig (Taylor and Francis, London, 1974), p. 1047.
[72]H. Rau, J. Chem Thermodyn. 6, 525 (1974).
[73]G. Weser, F. Hensel, and W. W. Warren, Jr., Ber. Bunsenges. Phys. Chem. 82, 588 (1978).
[74]D. J. Meschi and A. W. Searcy, J. Chem. Phys. 51, 5134 (1969).
[75]R. W. Schmutzler, Habilitation (University of Marburg, 1978) (unpublished).
[76]S. G. Bishop and P. C. Taylor, Solid State Commun. 11, 1323 (1972); see also, S. G. Bishop, in *Amorphous and Liquid Semiconductors,* edited by J. Stuke and W. Brenig (Taylor and Francis, London, 1974), p. 997.